Characteristics of Large-scale Structures in Turbulent Rayleigh-Bénard Convection in a Liquid Metal Layer

Takatoshi YANAGISAWA[1], Megumi AKASHI[2], Yuji TASAKA[2], Yuichi MURAI[2], Tobias VOGT[3] and Sven ECKERT[3]

[1] Japan Agency for Marine-Earth Science and Technology, 2-15 Natsushima-cho Yokosuka 237-0061, Japan
[2] Laboratory for Flow Control, Hokkaido University, Sapporo 060-8628, Japan
[3] Helmholtz Zentrum Dresden-Rossendorf, Dresden, Germany

We performed laboratory experiments on Rayleigh-Bénard convection with a liquid metal in a square box geometry having an aspect ratio five. Horizontal velocity profiles of convective flow were measured at several lines by using ultrasonic velocity profiling (UVP). By combining the information from profiles, we can reconstruct organized large-scale flow structures with turbulent fluctuations. Systematic variation of the structure was detected with increasing the Rayleigh number (Ra) from 10^4 to 10^5; a quasi-two-dimensional roll changes to a cell having a relatively larger horizontal scale. In addition, we found that the large-scale structure, whether it is roll or cell, show quasi-periodic oscillation whose representative period is approximately same as the circulation time of the large-scale flow. We also performed numerical simulations of convection with the same geometry as our experiments by setting a small Prandtl number (Pr=0.025) like a liquid metal. Quantitative comparison on the velocity profiles between experiments and simulations provided quite satisfactory agreement, and we analyzed the whole structure of the flow and the style of oscillation in detail based on the result of simulation.

Keywords: Rayleigh-Bénard convection, thermal turbulence, liquid metal, coherent structures, multi-dimensional measurement

1. Introduction

Rayleigh-Bénard convection (RBC) is an important problem in fluid dynamics and is also a basic configuration for various issues in geophysics, astrophysics and engineering. The RBC system is defined by the three dimensionless parameters, Rayleigh number (Ra), Prandtl number (Pr) and the aspect ratio of the fluid container (Γ). The convective flow structures were summarized on Ra-Pr parameter space and the convective flow reaches thermal turbulence regime for sufficiently large Ra depending on Pr [1]. Stable region of the two-dimensional (2D) steady roll structures on the Ra-wavenumber plane, named as "Busse balloon", was theoretically established for various Pr [2]. For very low Pr condition, $Pr \sim O(10^{-2})$, the Busse balloon shrinks into quite narrow area and the 2D rolls easily become time dependent slightly beyond the critical value of Ra as suggested by laboratory experiments [3]. Some numerical simulations demonstrated the behavior of travelling waves on the roll structures beyond the boundary of the Busse balloon until $Ra \sim 5 \times 10^3$ even with irregular time dependent flow [4]. Transitions to turbulence regime occurs with further increase of Ra and thus emergence of fully developed thermal turbulence are expected at relatively lower Ra values in low Pr convection compared with higher Pr fluids, such as air ($Pr \sim 1$) and water ($Pr \sim 7$). However, the process of the transitions to turbulence and the spatio-temporal characteristics of thermal turbulence in low Pr convection are not fully understood because liquid metals, representatives of very low Pr fluids, are opaque fluids and usual optical methods are not applicable.

Visualizations of the flow field in the opaque fluids have been realized by the ultrasonic velocity profiler (UVP) method [5] and UVP has been applied for investigations of thermal turbulence in low Pr convection. Instantaneous velocity distributions in convection of a cylindrical mercury layer were measured by UVP and complex coherent structures with periodic oscillations as called "large-scale circulations" were observed [6,7]. While the range of Ra is quite large in their studies, the aspect ratios of the fluid vessels are limited to around unity. The behaviors of RBCs of a liquid gallium layer under various intensities of a uniform imposed horizontal magnetic field in a square container with $\Gamma = 5$ have been investigated by our group [8]. Steady 2D roll patterns aligned parallel to the magnetic field under sufficiently strong intensities of the magnetic field change to the convection pattern having no principal direction under a weak or no magnetic field, and more complex, large-scale fluctuating patterns are observed. Investigations of the complex pattern are, however, limited in a narrow range of Ra and its spatio-temporal characteristics have not been elucidated.

The primary objective of this study is to reveal coherent structures connecting between the regular roll structures and the large-scale circulations in the low Pr turbulent convection confined by a square container with a moderate aspect ratio. The range of Ra is moderate, $O(10^4)$–$O(10^5)$, where convective flow reaches developed thermal turbulence at the maximum Ra. Multiple horizontal measurement lines of UVP were set perpendicularly at two heights in the fluid layer and three-dimensional (3D) flow structures were elucidated by combining the information from different profiles

https://doi.org/10.7795/810.20190809

obtained simultaneously. The experimental results were supplemented by direct numerical simulations and the comparison between them have developed understanding whole structures of turbulent flow in low *Pr* convection.

2. Apparatus and method

2.1 Experimental Setup

Schematic diagrams of the experimental setup, the square container filled with the fluid and arrangements of measurement lines of ultrasonic beams, are shown in Fig. 1, (a) top and (b) side view. The lateral walls of the vessel are made of 10-mm-thick PVC to attain thermal insulation. The fluid layer has a square horizontal cross section of 200 mm × 200 mm and a height of 40 mm, giving an aspect ratio of five. It is sandwiched between the top and bottom copper plates which ensure isothermal heating and cooling the system. The temperatures of each copper plate were controlled by water flow through channels inside the plates. *Ra* and *Pr* are described as

$$Ra = \frac{\beta g \Delta T L^3}{\nu \kappa} \cdots (1) \qquad Pr = \frac{\nu}{\kappa} \cdots (2)$$

Here, g, L and ΔT are gravitational acceleration, the height of the fluid layer and vertical temperature difference of the fluid layer, β, κ, and ν are thermal expansivity, thermal diffusivity and kinematic viscosity of the test fluid, respectively. The test fluid is the eutectic alloy of gallium, $Ga^{67}In^{20.5}Sn^{12.5}$ with $Pr = 0.03$ and the *Ra* can be controlled in the range from 7.9×10^3 to 1.0×10^5. UVP was adopted for obtaining instantaneous velocity profiles. Ten ultrasonic transducers with the basic frequency of 8 MHz were mounted horizontally in the holes at two side-walls of the vessel shown in Fig. 1 and contacted directly with the test fluid, where the gray lines in the figure indicate each measurement line crossing perpendicularly. Four transducers were set at 10 mm from the top plate (z = 30 mm) and other six transducers were set at 10 mm from the bottom plate (z = 10 mm). The temporal, spatial and velocity resolutions of the UVP measurements are 1.2 s, 1.4 mm and 0.5 mm/s, respectively. Measurements on the ten transducers were switched in time and velocity profiles along each measurement line were acquired sequentially. Thermistor (see T in Fig.1) was installed in the fluid layer 3mm below the top plate to measure temperature fluctuations with 10 Hz.

2.2 Method of numerical simulation

Direct numerical simulations are performed for the same geometry as experiments enclosed by no-slip velocity boundaries. The temperature is fixed at the top and bottom boundaries, while it is assumed to be adiabatic at side-walls. A set of governing equations are solved by the finite difference method with a uniform grid interval. The *Pr* is set as 0.025 to simulate a liquid metal. The detail of the simulation code is referred in [9].

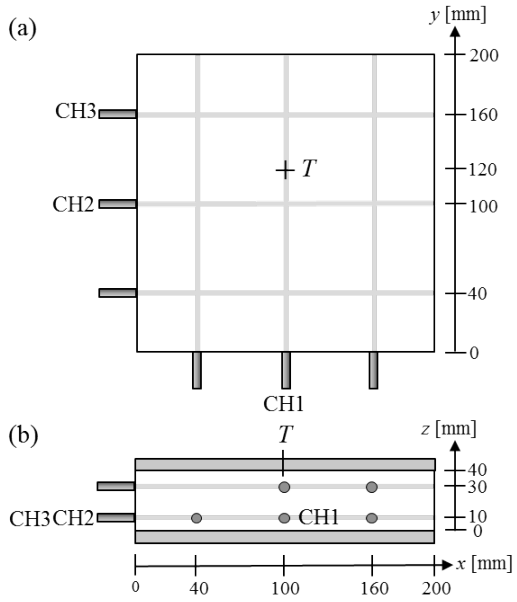

Figure 1: Experimental setup and arrangement of measurement lines: (a) top view and (b) side view, where gray lines indicate the measurement lines of UVP

3. Experimental results

Roll-like structures are observed at the lower range of *Ra* in this experiment as shown by spatio-temporal velocity maps in Fig. 2 (a,b), where velocity distribution was obtained parallel to the y-direction ((a) CH1) and the x-direction ((b) CH2) at $Ra = 7.9 \times 10^3$. The velocity maps (a) show wavy patterns with four stripes corresponding to four rolls whose time averaged axes are aligned parallel to the x-direction. Such pattern is commonly observed by other measurement lines parallel to the y-direction. The period of the oscillation is around 120 s and is the same order with the thermal diffusion time of the test fluid, $L^2/\kappa \approx 153$ s. The velocity map (b) shows patches, which are smaller than 30 mm and are synchronized with the wavy pattern observed in (a). The maximum velocity measured on the line of the x-direction is about half of that on the y-direction. This "four-roll structure" is stable and keeps the direction of roll axes throughout the measurement time once the structure emerges.

Fig. 2 (c,d) shows spatio-temporal velocity maps measured at $Ra = 2.1 \times 10^4$. Wavy patterns corresponding to four or three rolls with axes parallel to x- and y-direction are observed alternately in this flow state. In this flow state, roll-like structure corresponding to four-roll or three-roll aligned to the x- or y-direction are formed, but they are unstable and structures like rolls with a diagonal direction might be observed. And, they take transitions to different structures in some hundred seconds. It is understood as an intermediate regime from "four-roll structure" to the "three-roll structure", therefore, we defined this flow state as "four-three roll transitions".

Quasi-steady roll structures are observed again with the increase of *Ra* as shown in Fig. 2 (e,f) at $Ra = 4.4 \times 10^4$. The velocity map (f) shows a wavy pattern with three

stripes corresponding to three rolls parallel to the *y*-direction. The magnitude of velocity is larger than that in the lower *Ra*. And, the period of oscillation of the wavy pattern is shorter than that in the lower *Ra*.

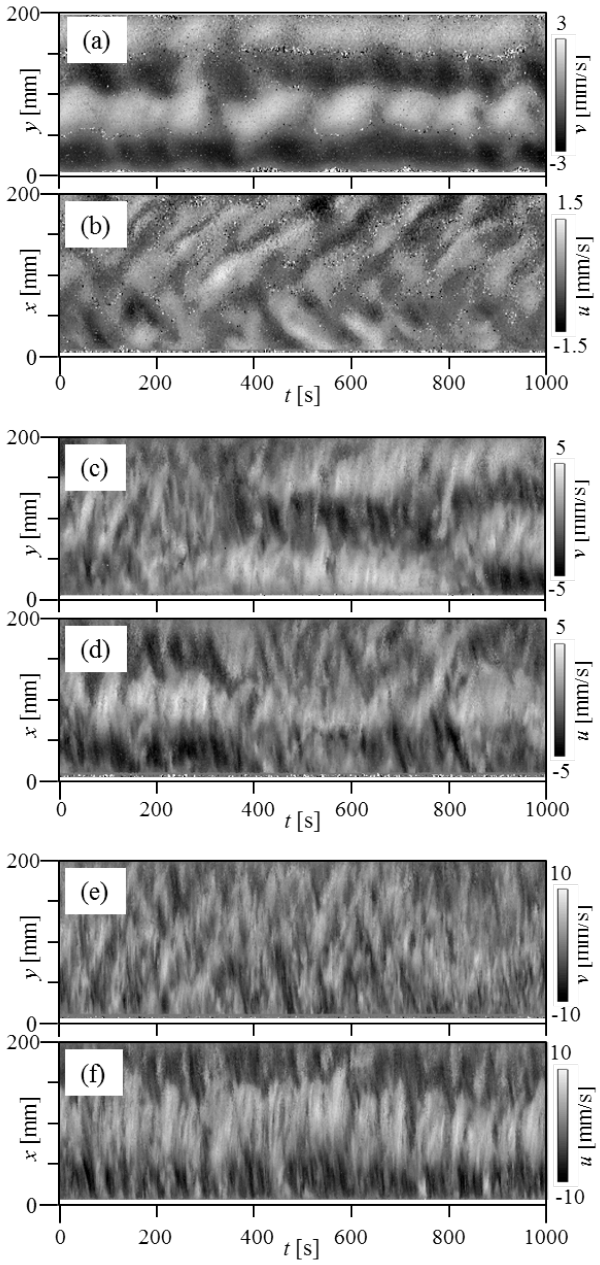

Figure 2: Spatio-temporal velocity distributions obtained on measurement lines CH1 and CH2 at (a,b) $Ra = 7.9\times10^3$, (c,d) $Ra = 2.1\times10^4$, (e,f) $Ra = 4.4\times10^4$

The velocity map (e) shows small patches oscillating synchronized with the wavy pattern. The maximum velocity measured in the *y*-direction is about 70% of that in the *x*-direction. This "three-roll structure" is quasi-stable and keeps the direction of roll axes for some thousand seconds, but sudden changes of the direction occur in a long duration.

The roll-like structure does not exist anymore at $Ra = 9.0 \times 10^4$ as shown in Fig. 3 (a,b). The velocity map (a) is obtained on the center lines parallel to the *y*-direction and shows a wavy band dividing the vessel into two parts. And, the velocity map on center lines to the *x*-direction shows similar flow patterns. The flow is heading for the center of the vessel from each wall side, hence, upwelling flow at the center is expected. The period of the oscillation is shorter than that in the former regime; it is almost the half of thermal diffusion time of the fluid layer. Fig. 3 (b) shows the velocity map obtained in the measurement line near the wall parallel to the *x*-direction and show patches dividing the layer length into three or four and oscillating with the same period as the wavy structure on the center lines. The velocity map near the wall parallel to the *y*-direction shows similar flow patterns. The magnitudes of velocities depend on the positions; the maximum velocities near the wall are about half of the values obtained on the center lines. The main structure is, therefore, a 3D wavy flow dividing the container into two parts. We named this flow state as "cell structure".

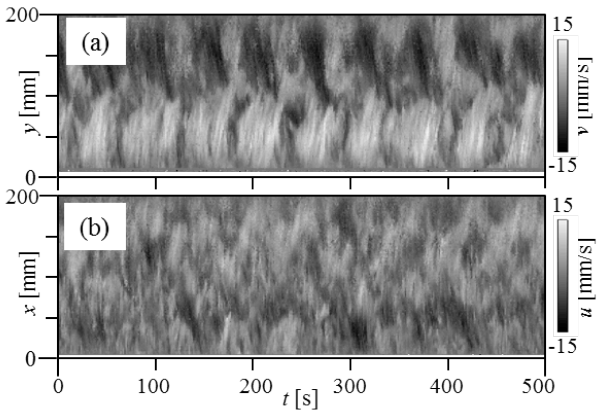

Figure 3: Spatio-temporal velocity distributions along (a) CH1 and (b) CH3 at $Ra = 9.0\times10^4$

The Rayleigh number dependence of the representative flow velocity U in this study can be summarized in a power law as $U(L/\kappa) = 0.1\ Ra^{0.5}$ throughout the structural transitions of flow. Typical oscillation frequencies f_{OS} have also systematic dependency on *Ra*, where the frequencies are defined as the frequency of the most energetic component in the spatial averaged power spectrum densities of velocity fluctuations. It can be expressed as $f_{OS}(L^2/\kappa) = 0.04\ Ra^{0.4}$. In Fig. 4, the typical period of wavy motions, $\tau = 1/f_{OS}$, is compared with the turn-over time, the time scale of the circulation of the fluid particle in flow structures. The turn-over time, τ_{TO}, is estimated in this system using the variable horizontal wavelength of the flow structure λ, the fluid layer thickness L, and flow velocity U as $\tau_{TO} = (2L+\lambda)/U$. Different symbols in Fig. 4 describe different flow regimes categorized above. A striking feature is that the ratio of τ to τ_{TO} takes values around unity through the studied range of *Ra*. This graph indicates that the oscillation period of observed wavy motion is comparable to the turn-over time of the flow, not only when the structure is roll-like but also when cell-like with developed thermal turbulence.

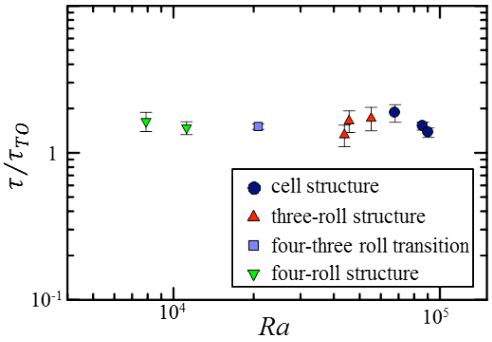

Figure 4: Plots of the periods of oscillation normalized by the turn-over times τ_{TO} with respect to *Ra*

4. Numerical simulations

We successfully reproduced in numerical simulations various behaviors observed in the experiment. Spatio-temporal velocity maps drawn by the data of simulations are useful for direct comparison with experiments, and Fig. 5 shows an example for a cell structure at $Ra = 1.0 \times 10^5$. The large-scale structure, together with the period of oscillation, is consistent with the result of the experiment shown in Fig. 3. The time scale is enlarged for five cycles of oscillation to identify fine structures in the flow. In Fig. 5 (a), we can see narrow oblique stripes in broad bands; they correspond to small vortices advected from the center to sides by the large-scale flow.

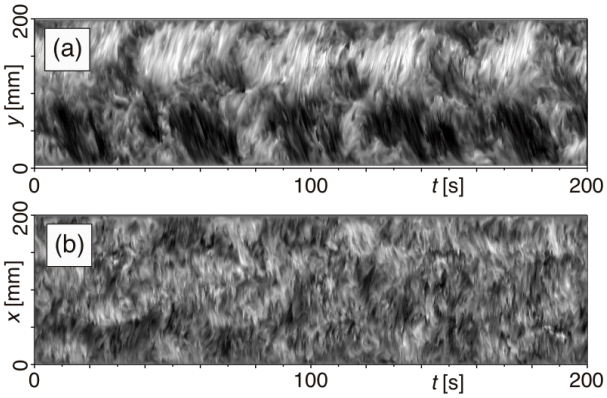

Figure 5: Numerical simulation: spatio-temporal velocity distributions obtained on lines CH1 and CH3. $Ra = 1.0 \times 10^5$

We can make up 3D image of flow structure from data sets of simulation. Two snapshots at different times are shown in Fig. 6 for the case of Fig. 5. They are indicated by isosurfaces of temperature. Temperature field is much more diffusive than velocity field due to low *Pr* of the fluid, hence isosurfaces of temperature are suitable to see a dominant structure. In this case, upwellings are located around the middle of four sides, while downwellings are located at the center and four corners of the container. While this basic cell-like structure is preserved throughout oscillations, the cell repeats expansion and shrink along *x*- and *y*-direction alternately. The oscillations observed in velocity profiles at center lines reflect this type of quasi-periodic motion of a cell.

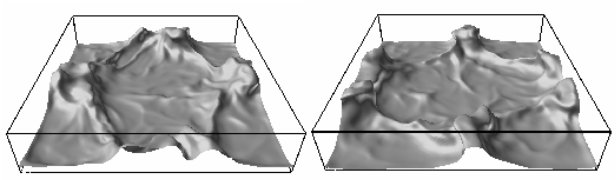

Figure 6: Numerical simulation: 3D view by an isosurface of the temperature. Snapshots at two moments indicating a style of oscillation for a cell-like structure. $Ra = 1.0 \times 10^5$

5. Summary

Transitions of flow structures in a low *Pr* convection were investigated by using a gallium alloy with multiple lines of UVP measurements. Distinct structures are observed in velocity profiles, those are roll-like up to $Ra \sim 6 \times 10^4$, while cell-like for the larger *Ra*. We found that both structures show quasi-regular periodicity in time. The typical periods of oscillation are comparable to the turn-over time of flow estimated by the measurement of velocity, and this relation holds throughout the transitions in the flow structure.

These transitions can be induced owing to the horizontal scale of the vessel, aspect ratio five. If the scale is short, flow structures are fixed to be roll-like or a single circulation. On the other hand, the cell-like structure and its oscillation observed in the present experiment is strongly constrained by the geometry of the square container. Experiments in wider geometries are expected in a future study to quantify natural horizontal scales of cell-like structures.

References

[1] Krishnamurti R: Some further studies on the transition to turbulent convection, J. Fluid Mech., 60 (1973), 285-303.
[2] Busse F.H: Non-linear properties of thermal convection, Rep. Prog. Phys., 41 (1978), 1929-1967.
[3] Rossby H.T: A study of Bénard convection with and without rotation, J. Fluid Mech., 36, (1969), 309-335.
[4] Nakano A, *et al.*: Numerical simulation of natural convection for a low-Prandtl-number fluid in a shallow rectangular region heated from below, Chem. Eng. J., 71 (1998), 175-182.
[5] Takeda Y (ed.): Ultrasonic Doppler Velocity Profiler for fluid flow, Springer (2012)
[6] Mashiko T, *et al.*: Instantaneous measurement of velocity fields in developed thermal turbulence in mercury, Phys. Rev. E, 69 (2004), 036306.
[7] Tsuji Y, *et al.*: Mean wind in convective turbulence of mercury, Phys. Rev. Lett., 94 (2005), 034501.
[8] Yanagisawa T, *et al.*: Convection patterns in a liquid metal under an imposed horizontal magnetic field, Phys. Rev. E, 88 (2013), 063020.
[9] Yanagisawa T, *et al.*: Flow reversals in low-Prandtl-number Rayleigh-Bénard convection controlled by horizontal circulations, Phys. Rev. E, 92 (2015), 023018.